Optical Chemical Sensor | Hot Paper

DOI: 10.1002/ange.201307217

A Noble-Metal-Free Porous Coordination Framework with Exceptional Sensing Efficiency for Oxygen**

Rui-Biao Lin, Fang Li, Si-Yang Liu, Xiao-Lin Qi, Jie-Peng Zhang, and Xiao-Ming Chen*

Oxygen sensors have a wide range of applications in food science, environmental analysis, space research, biochemistry among others.[1] Luminescence quenching[2] is a fast, high sensitivity, and simple oxygen sensing mechanism.[3] To serve as optical oxygen sensors, luminescent dyes must be dispersed in gas-permeable porous matrices.[4] According to the Stem–Volmer equation describing bimolecular collision quenching, long luminescence lifetimes (> 100 ns) are prerequisite for efficient quenching by oxygen, considering that the permeability of oxygen (i.e., the product of diffusion coefficient and solubility) is relatively low in common porous substrates.[5] Therefore, phosphorescent (originating from triplet excited states) coordination complexes of precious-metal ions, such as Pt^{II}, Pd^{II}, Ru^{II}, Au^{I}, Ir^{III}, Re^{I}, have been widely used as oxygen-sensing luminescent dyes.[2b]

Porous coordination polymers (PCPs) are highly ordered and porous matrices of metal complexes, which should be ideal for luminescent sensors.[6] Lin et al. demonstrated that the highly oxygen-sensitive phosphorescent complex [Ir(ppy)$_3$] (Hppy = 2-phenylpyridine) can be used as metalloligands to construct the first oxygen-sensing PCPs.[7] To date, only a few oxygen-sensing PCPs have been reported, which are all based on phosphorescent noble metal complexes.[7,8] While the sensitivities of phosphorescent PCPs are still moderate (< 88 % quenching at 1 bar O_2 or $I_0/I_{100} < 8.3$),[7,8] the requirement of large amounts of precious metals would seriously limits their applications. To reduce the materials cost, strategies, such as phosphorescence doping, have been introduced to reduce the precious-metal contents to somewhat lower levels.[8b,c] Nevertheless, no fluorescent or noble-metal-free PCP has been demonstrated to have oxygen sensing ability.[6a,b] Herein, we report a highly porous and fluorescent, noble-metal-free PCP with very high oxygen-sensing efficiency.

Solvothermal reaction of $Zn(NO_3)_2$, 2-aminoterephthalic acid (H_2abdc), and 3,3′,5,5′-tetramethyl-4,4′-bipyrazole (H_2bpz) in *N*,*N*-dimethylformamide and ethanol produced pale-yellow block crystals of $[Zn_4O(bpz)_2(abdc)]$·guest (MAF-X11, **1·g**; **g** = guest). Single-crystal structure analysis revealed that **1·g** is a non-interpenetrated **pcu** type coordination network composed of octahedral $\{Zn_4O(Rpz)_4(RCOO)_2\}$ (Rpz and RCOO denote pyrazolate and carboxylate groups, respectively) cores and two-connected bpz^{2-} and $abdc^{2-}$ linkers, which is isomorphous with $[Zn_4O(bpz)_2(bdc)]$ (MAF-X10, H_2bdc = 1,4-benzenedicarboxylic acid) (Figure 1 and Table S1).[9] MAF-X10 and MAF-X11 can be regarded as the analogues of $[Zn_4O(bdc)_3]$ (IRMOF-1) and $[Zn_4O(abdc)_3]$ (IRMOF-3),[10] respectively, in which two thirds of the dicarboxylate linkers are substituted by the bipyrazolate ligands. Although pyrazolate can adopt the same coordination mode as carboxylate, their metal–ligand bond lengths, bridging angles and lengths are clearly different, giving more-distorted Zn_4O clusters in MAF-X10 and MAF-X11 (Figure S1 and Table S2). Owing to the high symmetry of **1·g** ($P4_2/mcm$), the amino group of $abdc^{2-}$ is symmetrically disordered over four crystallography equivalent sites. Although the ligands are relatively short and contain many side groups,

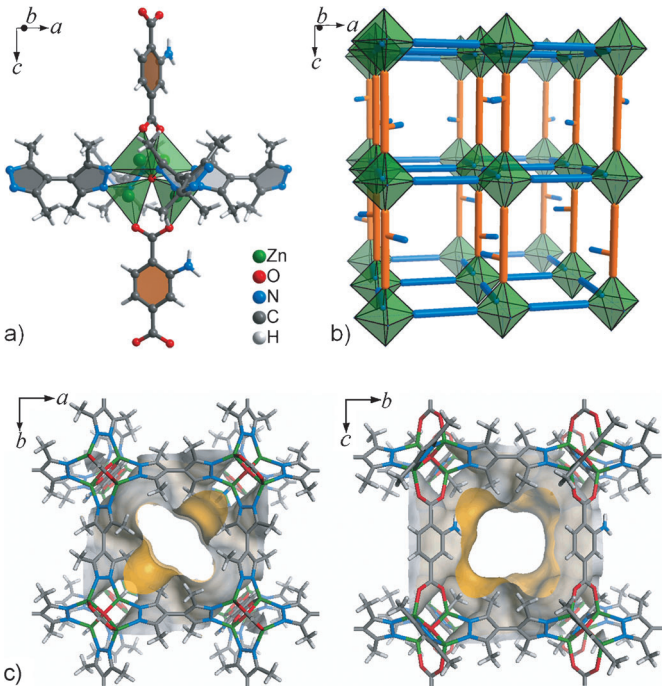

Figure 1. a) The $\{Zn_4O(Rpz)_4(RCOO)_2\}$ cluster, b) a simplified view of the 3D framework structure, and c) the pore surface structure viewed along two characteristic directions of **1**.

[*] R.-B. Lin, F. Li, S.-Y. Liu, X.-L. Qi, Prof. Dr. J.-P. Zhang, Prof. Dr. X.-M. Chen
MOE Key Laboratory of Bioinorganic and Synthetic Chemistry, State Key Laboratory of Optoelectronic Materials and Technologies
School of Chemistry and Chemical Engineering
Sun Yat-Sen University
Guangzhou 510275 (China)
E-mail: zhangjp7@mail.sysu.edu.cn

[**] This work was supported by the "973 Project" (2012CB821706), NSFC (21225105, 21121061, and 21001120) and the innovative talents training funded projects for Ph.D. students of Sun Yat-Sen University.

Supporting information for this article is available on the WWW under http://dx.doi.org/10.1002/anie.201307217.

1·g is still highly porous (void = 61.4%, ρ_{host} = 0.802 g cm^{-3}, Figure S2) with large pore size (cavity: 8.9 × 9.4 × 13.2 Å^3, apertures: 4.3 × 6.9 Å^2 along the *c*-axis and 5.5 × 5.8 Å^2 along the *a*-axis. The van der Waals radii are considered). To facilitate sample activation, **1·g** was soaked in EtOH to give **1·EtOH**. Thermogravimetry and powder X-ray diffraction of **1·EtOH** showed complete release of guest molecules at approximately 80 °C and framework decomposition at approximately 480 °C (Figure S3–S5), which is very high among PCPs.[11] In addition, guest-free **1** can retain most of its crystalline structure in air after 1 month (Figure S5), which is similar to its analogue MAF-X10.[12] In contrast, it is well known that the IRMOF structures are highly sensitive to moisture and easily collapse in air (e.g., under 1 h for IRMOF-1).[13] This difference can be explained by the strong coordination ability of pyrazolate groups and hydrophobic methyl groups.[14]

Under UV light, **1·EtOH** shows bright blue photoluminescence. The photoluminescence properties of **1·EtOH** (microcrystalline powder) and the free ligands (in dilute solutions) were investigated at room temperature. The excitation and emission spectra of **1·EtOH** are more like those of the free H_2abdc ligand rather than those of the free H_2bpz ligand (Figure 2), implying that the photoluminescence of **1·EtOH** mainly originates from the abdc^{2-} linkers. A small shoulder at around 425 nm can be identified in the emission spectrum, which may be assigned to small amounts of H_2abdc ligands adsorbed/coordinated on the outer crystal surface.[15] The red-shift of **1·EtOH** emission spectrum compared with that of H_2abdc can be attributed to the coordination effect.[16] As H_2bpz possesses a very small π-conjugation system, its maximum excitation and emission wavelengths are relatively short. Surprisingly, the desolvated compound **1** is highly luminescent in vacuum but barely luminescent in air. Considering the higher stability of **1**, it should not be destroyed by air. Indeed, the fluorescence of desolvated **1** can easily be recovered by adsorption of EtOH or placing it in vacuum. After testing a variety of gases, namely N_2, CO_2, and O_2 (the main components in air), it can be seen that the fluorescence of **1** is selectively quenched by O_2 (Figure 3a). The excitation and emission spectra of **1** in vacuum are very similar to those of **1·EtOH** (Figure S6). The fluorescence lifetimes of **1** (in vacuum) and **1·EtOH** are both composed of two components (Figure S7 and Table S3), and their average values are about 14.1 and 8.6 ns, respectively (Figure S7), which are much longer than those of the H_2abdc and H_2bpz in the solution state (< 2 ns, Table S3). The increased fluorescence lifetime is related to the high fluorescence intensity and can be explained by the reduction of nonradiative decays arising from molecular flexibility and interaction with solvent molecules.[17] Notably, the fluorescence lifetime of **1** is relatively long among coordination polymers.[18]

The photoluminescence of **1** was measured at different O_2 pressures, **1** showed an instant response and a stepwise change of emission intensity (Figure 3b,c). At 1 bar, the fluorescence (monitored at 470 nm) can be quenched by 96.5%, corresponding to I_0/I_{100} = 28.5. Linear fitting of the quenching data gave a Stern–Volmer constant K_{sv} of 27.1 bar^{-1} (Figure 3d). These values are significantly larger than for other oxygen-sensing phosphorescent PCPs and comparable with the highest values of hybrid materials composed of precious metal complexes (Table S4).[1c,7,8,19] Note that the intensity of the small shoulder (425 nm) decreases to a much smaller extent in O_2 than the main peak (470 nm) does, so that the

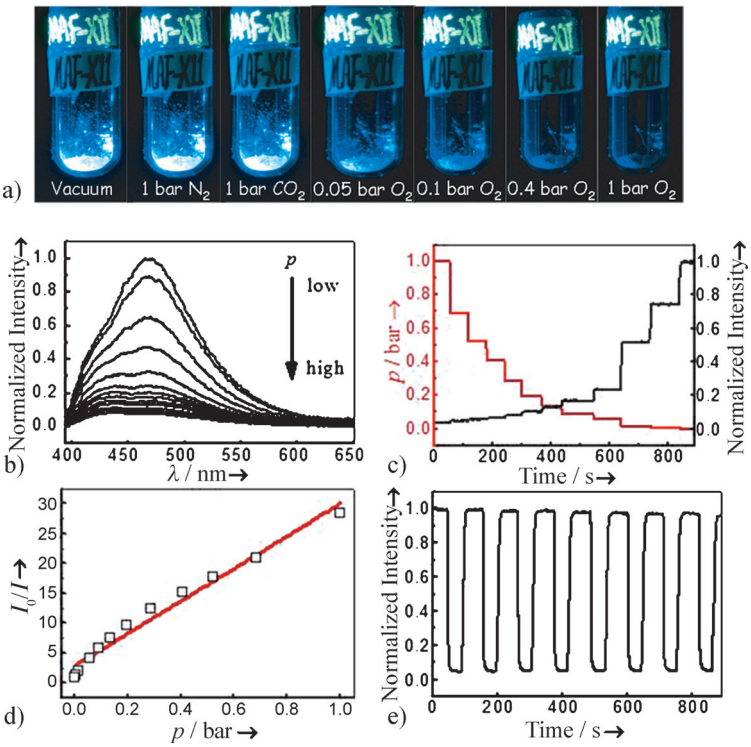

Figure 3. a) Photographs of **1** in different gas atmospheres under 365 nm UV light, b) emission spectra in different O_2 pressures (excitation at 345 nm), c) changes in luminescence intensity from vacuum to 1.0 bar O_2, d) Stern–Volmer plot, and e) reversible quenching/recovery of luminescence upon alternating exposure to O_2 and vacuum for **1**.

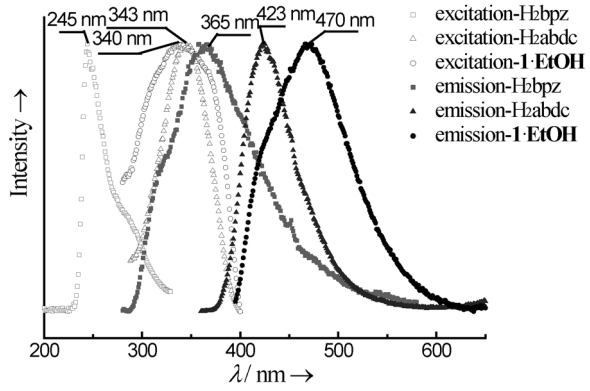

Figure 2. Photoluminescence spectra of microcrystalline **1·EtOH** and ethanol solutions of H_2bpz and H_2abdc.

emission peak shows an apparent blue-shift. This phenomenon is consistent with the quite different fluorescence lifetimes of the two emission components (Figure S7 and Table S3). The change of fluorescence intensity of **1** was monitored for alternating cycles at 1 bar O_2 and vacuum, which indicated that the quenching response is rapid, reversible, and highly stable (Figure 3e). To examine more practical performance, the fluorescence response was further measured using air as the quencher. As shown in Figure S8, the quenching efficiencies in air are similar with that in pure O_2 at $p = 0.21$. This observation showed that the oxygen-sensing efficiency of **1** is not influenced by other components in air, which further illustrates the O_2 selectivity.

Although oxygen-quenching fluorescence has not been reported for PCPs yet, similar phenomena are well known for many fluorescent organic molecules with lifetimes in the range of 1–100 ns (such as aromatic derivatives).[20] The efficient quenching of fluorescence coming from a singlet excited state can be explained by several quenching pathways (Scheme S1).[20,21] Nevertheless, the oxygen quenching of fluorescence in organic molecules is only effective in the solution and gaseous states. Generally, their quenching efficiencies become extremely low in the solid state or when dispersed in porous matrixes, as the oxygen permeabilities are only 0.1–1 % of those in the solution and gaseous states.[5]

To understand the high and rapid fluorescence quenching of **1**, N_2 and O_2 sorption experiments were performed (Figure 4a). The N_2 sorption isotherm at 77 K exhibits a type-I character with a saturated uptake 428 cm^3 (standard temperature and pressure; STP) g^{-1}, corresponding to a pore volume of 0.67 $cm^3 g^{-1}$ (0.77 $cm^3 g^{-1}$ calculated from the crystal structure). At 77 K, the saturated uptake of O_2 is 598 cm^3 (STP) g^{-1}, corresponding to a pore volume of 0.75 $cm^3 g^{-1}$, which is higher than for the N_2 isotherm and very close to the theoretical one. The BET and Langmuir surface areas were calculated to be 1495 and 1796 $m^2 g^{-1}$ by using the N_2 isotherm, and 2091 and 2341 $m^2 g^{-1}$ by the O_2 isotherm, respectively. The Horvath–Kawazoe model calculation indicates a pore-diameter distribution centered at 7.3 Å from the N_2 isotherm (Figure S9) or 10.3 Å from the O_2 isotherm (Figure 4b). These data indicate that O_2 with a smaller molecular size can fill the undulating pore surfaces of **1** more effectively.

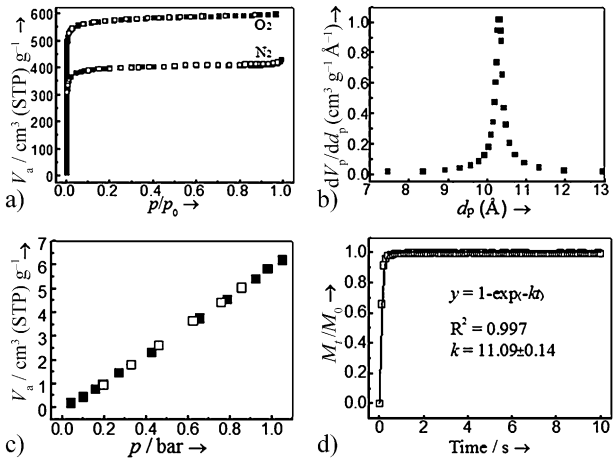

Figure 4. a) N_2 and O_2 adsorption (solid) and desorption (open) isotherms at 77 K, b) pore size distribution (Horvath–Kawazoe model) calculated from the 77 K O_2 adsorption isotherm, c) O_2 adsorption (solid) and desorption (open) isotherm at 298 K, and d) kinetic profile of O_2 adsorption at 298 K (the line represents the exponential fit) for **1**.

Further sorption experiment showed high uptake and very fast sorption kinetics for O_2 at 298 K (Figure 4c,d). The O_2 sorption isotherm at 298 K exhibits a linear character, indicating a weak binding affinity between O_2 and pore surfaces of **1** because O_2 has a very low boiling point and is supercritical at this temperature. Nevertheless, the O_2 adsorption amount reaches 5.9 cm^3 (STP) g^{-1} at 1 bar, being equivalent to a solubility of 0.21 mol L^{-1}, which is much higher than the highest values of solvents and solid porous matrixes used for oxygen-sensing (8×10^{-3} mol L^{-1} for ethyl cellulose).[22] The adsorption/desorption can reach equilibrium within 1 s, giving a large diffusion coefficient 1.8×10^{-5} $cm^2 s^{-1}$ (Figure 4d and Figure S10), which is similar to those of highly porous PCPs, such as IRMOF-1[23] and significantly higher than those of oxygen-permeating polymers, such as aromatic derivative-labeled polystyrene films ($2.8–5.3 \times 10^{-7}$ $cm^2 s^{-1}$)[24] and fluorothiophenyl modified polyvinyl chloride membranes ($1.8–4.1 \times 10^{-8}$ $cm^2 s^{-1}$),[25] and comparable with those of mesoporous nanocomposites of silicone resin/inorganic filler ($0.05–3.6 \times 10^{-5}$ $cm^2 s^{-1}$).[5,26] Based on the solubility and diffusion coefficient values of **1**, its oxygen permeability can be calculated as 3.8×10^{-9} mol $cm^{-1} s^{-1} bar^{-1}$, which is 2–4 orders of magnitude higher than for other solid porous matrixes ($10^{-13}–10^{-11}$ mol $cm^{-1} s^{-1} bar^{-1}$),[5,26] which accounts for its unexpectedly high oxygen-sensing efficiency considering the relatively short fluorescence lifetime compared with phosphorescent dyes.

For comparison, we also checked the fluorescence properties of IRMOF-1, IRMOF-3, and MAF-X10, which showed emission peaks centered at 396 nm,[27] 452 nm,[28] and 407 nm,[9] respectively (Figure S11). The fluorescence intensities of these compounds are clearly weaker than that of MAF-X11 (Figure S12). An increase in the extent of the π-conjugation system, such as from bdc^{2-} to $abdc^{2-}$, generally leads to a shift of fluorescence spectra to longer wavelengths and an increase in fluorescence intensity (quantum yield).[29] Compared with IRMOF-1 and IRMOF-3, the red-shifted emission spectra of MAF-X10 and MAF-X11 may be attributed to the differences in the coordination and electronic structures of the Zn_4O clusters (Figure S1 and Table S2), which lead to different perturbation effect on the excited-state structure and energy of the carboxylate fluorophore.[16] Further, the fluorophores (carboxylate linkers) in IRMOF-1 and IRMOF-3 form close contacts with each other (O···O 3.1 Å), which promotes energy transfer of excited states and non-radiative decay.[29] On the other hand, the shortest contacts between adjacent fluorophores in MAF-X10 and MAF-X11 are much longer (O···O 6.1 Å), because the dicarboxylate linkers are separated by bipyrazolate ligands. Although the carboxylate and pyrazolate linkers form close contacts, the very small π-conjugation system of a pyrazolate

ring (two pyrazolate rings in bpz^{2-} have a dihedral angle of about 80°) makes its excitation energy gap too large to accept the excitation energy of the dicarboxylate ligands.[29] Preliminary experiments showed that the fluorescence of these PCPs can be also quenched by O_2, although their quenching efficiencies were lower than for MAF-X11 (Figure S11), being consistent with their weak fluorescence intensity (short life-time).[17a] This observation indicates that fluorescence quenching by O_2 might be found in many base-metal PCPs, but the weak un-quenched fluorescence, low quenching efficiency, and/or air instability of common PCPs have prevented the discovery of such a useful property.

In summary, we demonstrated that a highly porous and fluorescent PCP constructed from Zn^{II} ions as the sole metal component can show an exceptionally high oxygen-sensing efficiency. In principle, the fluorescence of PCPs can be quenched by O_2 by many well-established pathways/mechanisms as for fluorescent organic molecules, but oxygen-sensing fluorescent PCP was unprecedented until now, which should be probably attributed to the instability in air of PCPs, their weak fluorescence intensity (short lifetimes), and/or poor oxygen permeability. For MAF-X11, the unique framework structure not only provides high oxygen permeability, but also allows the fluorophores to be well isolated from each other to avoid self-quenching and give relatively long fluorescence lifetimes. These results may inspire future design and fabrication of novel low-cost optical oxygen-sensing materials.

Experimental Section

$[Zn_4O(bpz)_2(abdc)]$·guest (**1·g**, MAF-X11). A mixture of H_2abdc (0.068 g, 0.375 mmol), H_2bpz (0.143 g, 0.75 mmol), $Zn(NO_3)_2{\cdot}6H_2O$ (0.446 g, 1.5 mmol), *N*,*N*-dimethylformamide (30 mL), and EtOH (20 mL) was placed in a Teflon-lined stainless steel vessel (100 mL) and heated at 120 °C for 72 h, and then it was cooled to room temperature at a rate of 0.1 °C min^{-1}. The resulting pale-yellow block polycrystals (Figure S5) of **1·g** were isolated by decanting and treated with ethanol and dried under vacuum (yield 203 mg, 45 %). Single crystals for X-ray single-crystal diffraction were prepared by heating a solution of H_2abdc (0.009 g, 0.025 mmol), H_2bpz (0.010 g, 0.05 mmol), and $Zn(NO_3)_2{\cdot}6H_2O$ (0.030 g, 0.10 mmol) in a mixed solvent of *N*,*N*-dimethylformamide and EtOH ($v/v = 2/1$, 3 mL) in a sealed glass tube (1.0 cm o.d. × 10 cm length) at 130 °C for 72 h, and then the mixture was cooled to room temperature at a rate of 0.1 °C min^{-1} to give pale-yellow block single crystals (25 mg, yield 84 %). Elemental analysis: Calcd for $C_{29.2}H_{34.6}Zn_4N_9O_{6.6}$ ($[Zn_4O(bpz)_2(abdc)]{\cdot}H_2O{\cdot}0.6$ EtOH): C 39.90, H 3.97, N 14.34. Found: C 39.92, H 3.85, N 14.26 %. IR (KBr): $\tilde{\nu}$ =3464m, 2925m, 1668vs, 1562s, 1495m, 1440s, 1385s, 1257m, 1095m, 1052s, 820w, 770m, 662w, 558w cm^{-1}.

Received: August 16, 2013
Published online: October 16, 2013

Keywords: fluorescence · luminescence · metal–organic framework · oxygen sensing · quenching

[1] a) A. Persson, E. Gross, P. Laurent, K. E. Busch, H. Bretes, M. de Bono, *Nature* **2009**, *458*, 1030 – 1033; b) S. E. J. Williams, P. Wootton, H. S. Mason, J. Bould, D. E. Iles, D. Riccardi, C. Peers, P. J. Kemp, *Science* **2004**, *306*, 2093 – 2097; c) C.-F. Wu, B. Bull, K. Christensen, J. McNeill, *Angew. Chem.* **2009**, *121*, 2779 – 2783; *Angew. Chem. Int. Ed.* **2009**, *48*, 2741 – 2745.

[2] a) X.-J. Zhu, S.-T. Fu, W.-K. Wong, J.-P. Guo, W.-Y. Wong, *Angew. Chem.* **2006**, *118*, 3222 – 3226; *Angew. Chem. Int. Ed.* **2006**, *45*, 3150 – 3154; b) Q. Zhao, F.-Y. Li, C.-H. Huang, *Chem. Soc. Rev.* **2010**, *39*, 3007 – 3030.

[3] C. McDonagh, C. S. Burke, B. D. MacCraith, *Chem. Rev.* **2008**, *108*, 400 – 422.

[4] D. E. Achatz, R. J. Meier, L. H. Fischer, O. S. Wolfbeis, *Angew. Chem.* **2011**, *123*, 274 – 277; *Angew. Chem. Int. Ed.* **2011**, *50*, 260 – 263.

[5] X. Lu, M. A. Winnik, *Chem. Mater.* **2001**, *13*, 3449 – 3463.

[6] a) L. E. Kreno, K. Leong, O. K. Farha, M. Allendorf, R. P. Van Duyne, J. T. Hupp, *Chem. Rev.* **2012**, *112*, 1105 – 1125; b) Y.-J. Cui, Y.-F. Yue, G.-D. Qian, B.-L. Chen, *Chem. Rev.* **2012**, *112*, 1126 – 1162; c) H.-L. Jiang, Y. Tatsu, Z.-H. Lu, Q. Xu, *J. Am. Chem. Soc.* **2010**, *132*, 5586 – 5587; d) S. Pramanik, C. Zheng, X. Zhang, T. J. Emge, J. Li, *J. Am. Chem. Soc.* **2011**, *133*, 4153 – 4155; e) N. Yanai, K. Kitayama, Y. Hijikata, H. Sato, R. Matsuda, Y. Kubota, M. Takata, M. Mizuno, T. Uemura, S. Kitagawa, *Nat. Mater.* **2011**, *10*, 787 – 793; f) Y. Takashima, V. M. Martínez, S. Furukawa, M. Kondo, S. Shimomura, H. Uehara, M. Nakahama, K. Sugimoto, S. Kitagawa, *Nat. Commun.* **2011**, *2*, 168; g) K. C. Stylianou, R. Heck, S. Y. Chong, J. Bacsa, J. T. A. Jones, Y. Z. Khimyak, D. Bradshaw, M. J. Rosseinsky, *J. Am. Chem. Soc.* **2010**, *132*, 4119 – 4130; h) B. V. Harbuzaru, A. Corma, F. Rey, P. Atienzar, J. L. Jordá, H. García, D. Ananias, L. D. Carlos, J. Rocha, *Angew. Chem.* **2008**, *120*, 1096 – 1099; *Angew. Chem. Int. Ed.* **2008**, *47*, 1080 – 1083; i) H.-J. Son, S.-Y. Jin, S. Patwardhan, S. J. Wezenberg, N. C. Jeong, M. So, C. E. Wilmer, A. A. Sarjeant, G. C. Schatz, R. Q. Snurr, O. K. Farha, G. P. Wiederrecht, J. T. Hupp, *J. Am. Chem. Soc.* **2013**, *135*, 862 – 869; j) C. A. Kent, D.-M. Liu, T. J. Meyer, W.-B. Lin, *J. Am. Chem. Soc.* **2012**, *134*, 3991 – 3994; k) B.-L. Chen, L.-B. Wang, F. Zapata, G.-D. Qian, E. B. Lobkovsky, *J. Am. Chem. Soc.* **2008**, *130*, 6718 – 6719; l) J.-H. Wang, M. Li, D. Li, *Chem. Sci.* **2013**, *4*, 1793 – 1801; m) A.-J. Lan, K.-H. Li, H.-H. Wu, D. H. Olson, T. J. Emge, W. Ki, M.-C. Hong, J. Li, *Angew. Chem.* **2009**, *121*, 2370 – 2374; *Angew. Chem. Int. Ed.* **2009**, *48*, 2334 – 2338; n) X.-L. Qi, R.-B. Lin, Q. Chen, J.-B. Lin, J.-P. Zhang, X.-M. Chen, *Chem. Sci.* **2011**, *2*, 2214 – 2218; o) Y. Cui, H. Xu, Y. Yue, Z. Guo, J. Yu, Z. Chen, J. Gao, Y. Yang, G. Qian, B. Chen, *J. Am. Chem. Soc.* **2012**, *134*, 3979 – 3982.

[7] Z.-G. Xie, L.-Q. Ma, K. E. deKrafft, A. Jin, W.-B. Lin, *J. Am. Chem. Soc.* **2010**, *132*, 922 – 923.

[8] a) M.-L. Ho, Y.-A. Chen, T.-C. Chen, P.-J. Chang, Y.-P. Yu, K.-Y. Cheng, C.-H. Shih, G.-H. Lee, H.-S. Sheu, *Dalton Trans.* **2012**, *41*, 2592 – 2600; b) S. M. Barrett, C. Wang, W.-B. Lin, *J. Mater. Chem.* **2012**, *22*, 10329 – 10334; c) X.-L. Qi, S.-Y. Liu, R.-B. Lin, P.-Q. Liao, J.-W. Ye, Z. Lai, Y. Guan, X.-N. Cheng, J.-P. Zhang, X.-M. Chen, *Chem. Commun.* **2013**, *49*, 6864 – 6866; d) J. An, C. M. Shade, D. A. Chengelis-Czegan, S. Petoud, N. L. Rosi, *J. Am. Chem. Soc.* **2011**, *133*, 1220 – 1223.

[9] L. Hou, Y.-Y. Lin, X.-M. Chen, *Inorg. Chem.* **2008**, *47*, 1346 – 1351.

[10] M. Eddaoudi, J. Kim, N. Rosi, D. Vodak, J. Wachter, M. O'Keeffe, O. M. Yaghi, *Science* **2002**, *295*, 469 – 472.

[11] Z.-Y. Gu, C.-X. Yang, N. Chang, X.-P. Yan, *Acc. Chem. Res.* **2012**, *45*, 734 – 745.

[12] a) A. Nalaparaju, J. W. Jiang, *Langmuir* **2012**, *28*, 15305 – 15312; b) A. Nalaparaju, X. S. Zhao, J. W. Jiang, *Energy Environ. Sci.* **2011**, *4*, 2107 – 2116.

[13] a) J. G. Nguyen, S. M. Cohen, *J. Am. Chem. Soc.* **2010**, *132*, 4560 – 4561; b) S. J. Yang, J. Y. Choi, H. K. Chae, J. H. Cho, K. S. Nahm, C. R. Park, *Chem. Mater.* **2009**, *21*, 1893 – 1897.

[14] J.-P. Zhang, Y.-B. Zhang, J.-B. Lin, X.-M. Chen, *Chem. Rev.* **2012**, *112*, 1001 – 1033.
[15] M. Kondo, S. Furukawa, K. Hirai, S. Kitagawa, *Angew. Chem.* **2010**, *122*, 5455 – 5458; *Angew. Chem. Int. Ed.* **2010**, *49*, 5327 – 5330.
[16] S.-L. Zheng, X.-M. Chen, *Aust. J. Chem.* **2004**, *57*, 703 – 712.
[17] a) E. L. Wehry in *Instrumental Techniques for analytical chemistry* (Ed.: F. A. Settle), Prentice Hall, Upper Saddle River, NJ, **1997**, pp. 507 – 539; b) M. D. Allendorf, C. A. Bauer, R. K. Bhakta, R. J. T. Houk, *Chem. Soc. Rev.* **2009**, *38*, 1330 – 1352.
[18] a) N. B. Shustova, B. D. McCarthy, M. Dincă, *J. Am. Chem. Soc.* **2011**, *133*, 20126 – 20129; b) C. A. Bauer, T. V. Timofeeva, T. B. Settersten, B. D. Patterson, V. H. Liu, B. A. Simmons, M. D. Allendorf, *J. Am. Chem. Soc.* **2007**, *129*, 7136 – 7144.
[19] a) M. T. Murtagh, M. R. Shahriari, M. Krihak, *Chem. Mater.* **1998**, *10*, 3862 – 3869; b) L. Huynh, Z. Wang, J. Yang, V. Stoeva, A. Lough, I. Manners, M. A. Winnik, *Chem. Mater.* **2005**, *17*, 4765 – 4773; c) X.-D. Wang, X. Chen, Z.-X. Xie, X.-R. Wang, *Angew. Chem.* **2008**, *120*, 7560 – 7563; *Angew. Chem. Int. Ed.* **2008**, *47*, 7450 – 7453; d) B. W.-K. Chu, V. W.-W. Yam, *Langmuir* **2006**, *22*, 7437 – 7443.
[20] R. G. Brown, D. Phillips, *J. Chem. Soc. Faraday Trans.* **1974**, *70*, 630 – 636.
[21] a) W. M. Nau, J. C. Scaiano, *J. Phys. Chem.* **1996**, *100*, 11360 – 11367; b) C. Schweitzer, R. Schmidt, *Chem. Rev.* **2003**, *103*, 1685 – 1758.
[22] A. Mills, *Sens. Actuators B* **1998**, *51*, 60 – 68.
[23] Z.-X. Zhao, X.-L. Ma, Z. Li, Y.-S. Lin, *J. Membr. Sci.* **2011**, *382*, 82 – 90.
[24] J. E. Guillet, M. Andrews, *Macromolecules* **1992**, *25*, 2752 – 2756.
[25] K. Bierbrauer, M. López-González, E. Riande, C. Mijangos, *J. Membr. Sci.* **2010**, *362*, 164 – 171.
[26] C. N. Jayarajah, A. Yekta, I. Manners, M. A. Winnik, *Macromolecules* **2000**, *33*, 5693 – 5701.
[27] P. L. Feng, J. J. Perry Iv, S. Nikodemski, B. W. Jacobs, S. T. Meek, M. D. Allendorf, *J. Am. Chem. Soc.* **2010**, *132*, 15487 – 15489.
[28] R. M. Abdelhameed, L. D. Carlos, A. M. S. Silva, J. Rocha, *Chem. Commun.* **2013**, *49*, 5019 – 5021.
[29] B. Valeur in *Molecular Fluorescence: Principles and Applications*, Wiley-VCH, Weinheim, **2001**, pp. 34 – 71.

